MITNE-235

A STATIC, TWO-PHASE, THERMAL HYDRAULIC FEEDBACK MODEL FOR THE NODAL CODE QUANDRY

by

Hussein Khalil
Department of Nuclear Engineering

July 31, 1980

One of the goals of the on-going research for the EPRI is to develop efficient neutronic calculational methods that are applicable to fuel management problems (e.g., depletion, fuel shuffling). An important consideration in this effort is to account for reactor thermal-hydraulic feedback effects, which are known to affect significantly the neutron cross-sections of the various materials in the reactor. In addition, it must be demonstrated that the neutronic solution method is not affected adversely by the non-linearity introduced by the thermal-hydraulic feedback (i.e., by flux-dependent cross sections). To allow for these feedback effects, the simple WIGL thermal-hydraulic model [1] was incorporated into the computer code QUANDRY [2], which would perform the neutronic calculations in the overall fuel management model.

Unfortunately, the existing WIGL model assumes that no boiling of the coolant occurs and is thus incapable of simulating the significant cross section feedback in BWR's that results from the greatly reduced coolant density associated with boiling. For this reason, the WIGL model has been extended to the static boiling case to verify the accuracy, convergence, and stability of the neutronic solution in QUANDRY in cases where boiling takes place. This extended WIGL model was proposed by Professor J.F. Meyer and has been recently implemented in QUANDRY. In this paper, the extension of the WIGL model to the steady-state boiling case is presented, results of its application to a simple test problem are given, and conclusions about the effect of boiling on the neutronic calculations are drawn.

Model Development

In the WIGL model, three quantities are of interest in each node (i,j,k): the average fuel temperature $\overline{T}^f_{ijk}$, the average moderator temperature $\overline{T}^c_{ijk}$, and the average moderator density $\overline{\rho}^c_{ijk}$.

Equations for the fuel and moderator temperatures are derived by performing time-dependent energy balances on the fuel and coolant in each node. These equations may be written as [2]

$$\frac{d\bar{T}^f_{ijk}}{dt} = \frac{1}{\rho^f C^f}\left\{(1-n)q'''_{ijk} - \frac{V^c_{ijk}}{V^f_{ijk}}\left[\frac{1}{A_h U} + \frac{1}{A_h h_o (W/W_o)^{0.8}}\right]^{-1}(\bar{T}^f_{ijk} - \bar{T}^c_{ijk})\right\} \tag{1}$$

$$\frac{d\bar{T}^c_{ijk}}{dt} = \left(\frac{\partial \rho^c H}{\partial \bar{T}^c}\right)^{-1}\left\{\left[\frac{1}{A_h U} + \frac{1}{A_h h_o (W/W_o)^{0.8}}\right]^{-1}(\bar{T}^f_{ijk} - \bar{T}^c_{ijk}) + \frac{2W^n_{ijk}C^c}{V^c_{ijk}}(T^b_{ijk} - \bar{T}^c_{ijk}) + n q'''_{ijk}\frac{V^f_{ijk}}{V^c_{ijk}}\right\} \tag{2}$$

$i = 1, \ldots, NX$

$j = 1, \ldots, NY$

$k = 1, \ldots, NZ$

where $$\bar{T}^c_{ijk} = \frac{1}{2}(T^b_{ijk} + T^b_{ijk+1}) \tag{3}$$

and where the notation is the same as that of Smith [2].

This paper treats only the static form of these equations. With the steady state assumption, Eq. (1) becomes

$$\bar{T}^f_{ijk} - \bar{T}^c_{ijk} = \frac{V^f_{ijk}}{V^c_{ijk}}(R_1 + R_2)(1-n)q'''_{ijk} \tag{4}$$

where $R_1 \equiv (A_h U)^{-1}$ and $R_2 = [A_h h_o (W/W_o)^{0.8}]^{-1}$.

Similarly, Eq. (2) becomes

$$\bar{T}^f_{ijk} - \bar{T}^c_{ijk} = -(R_1 + R_2)\left[\frac{2W^n_{ijk}C^c}{V^c_{ijk}}(T^b_{ijk} - \bar{T}^c_{ijk}) + n q'''_{ijk}\frac{V^f_{ijk}}{V^c_{ijk}}\right] . \tag{5}$$

Substitution for $\bar{T}^f_{ijk} - \bar{T}^c_{ijk}$ from Eq. (4) into Eq. (5) gives

$$\bar{T}^c_{ijk} = T^b_{ijk} + \frac{V^f_{ijk}\, q'''_{ijk}}{2W^\Delta_{ijk}\, C^c} \quad .$$

Elimination of $\bar{T}^c_{ijk}$ using Eq. (3) yields

$$T^b_{ijk+1} - T^b_{ijk} = \frac{V^f_{ijk}\, q'''_{ijk}}{C^c\, W^\Delta_{ijk}} \quad .$$

This equation may be rewritten in terms of the coolant specific enthalpy (enthalpy per unit mass) H as

$$H_{ijk+1} - H_{ijk} = \frac{V^f_{ijk}\, q'''_{ijk}}{W^\Delta_{ijk}} \quad . \qquad (6)$$

If the inlet enthalpy H_{ij1} (i=1, ..., NX; j=1, ..., NY) is specified, H_{ijk} can be determined successively for all values of k (k=1, ..., NZ) using Eq. (6). If the enthalpy is assumed to vary linearly with axial position within the node, the average enthalpy in each node is given by

$$\bar{H}_{ijk} = \frac{1}{2}\left(H_{ijk+1} + H_{ijk}\right) \quad .$$

The average coolant temperature $\bar{T}^c_{ijk}$ can thus be calculated from

$$\bar{T}^c_{ijk} = T_{sat} - \frac{H_f - \bar{H}_{ijk}}{C^c} \qquad \text{(use for } \bar{H}_{ijk} < H_f\text{)} \qquad (7)$$

where T_{sat} is the saturation temperature, and H_f is the enthalpy of the saturated liquid. If $\bar{H}_{ijk}$ exceeds H_f, the average coolant temperature is set equal to the saturation temperature, i.e.

$$\bar{T}^c_{ijk} = T_{sat} \qquad \text{(use for } \bar{H}_{ijk} \geq H_f\text{)} . \qquad (8)$$

Thus it is assumed that no superheating of the coolant takes place.

Once the average coolant temperature in a given node is known, the average fuel temperature is determined directly using Eq. (4) as

$$\bar{T}^f_{ijk} = \bar{T}^c_{ijk} + \frac{V^f_{ijk}}{V^c_{ijk}} (R_1 + R_2)(1-\lambda) q'''_{ijk} . \qquad (9)$$

To avoid the possible jump in $\bar{T}^f$ as $\bar{T}^c$ reaches T_{sat}, $\bar{T}^f$ is evaluated as the minimum of $\bar{T}^f$ in Eq. (9) and

$$\bar{T}^f_{ijk} = T_{sat} + \frac{V^f_{ijk}}{V^c_{ijk}} R_1 (1-\lambda) q'''_{ijk} . \qquad (10)$$

This latter expression implies that the fuel cladding is at the saturation temperature.

To evaluate the average coolant density in node (i,j,k), three distinct cases are considered: 1) $H_{ijk+1} \leq H_f$ (the entire node is subcooled), 2) $H_{ijk} \geq H_f$ (boiling occurs for all z within the node), 3) $H_{ijk} < H_f < H_{ijk+1}$ (boiling begins within the node). Each of these cases is considered separately below.

Case 1) ($H_{ijk+1} \leq H_f$). In this case, the assumption is made that the coolant density decreases linearly with enthalpy H for values of H between H_{ij1} and H_f. If the inlet density ρ^c_{ij1} is known, the coolant density at successive axial points can thus be computed from

$$\rho^c_{ijk+1} = \rho^c_{ijk} + \frac{\rho_f - \rho^c_{ijk}}{H_f - H_{ijk}} \left(H_{ijk+1} - H_{ijk} \right) \tag{11}$$

where ρ^f is the density of the saturated liquid. If it is additionally assumed that the coolant enthalpy varies linearly with axial position in a given node, the average coolant density in node (i,j,k) is given by

$$\bar{\rho}^c_{ijk} = \frac{1}{H_{ijk+1} - H_{ijk}} \int_{H_{ijk}}^{H_{ijk+1}} \rho^c(H)\, dH$$

Substitution of $\rho^c(H) = \rho^c_{ijk} + (\rho^f - \rho^c_{ijk})(H - H_{ijk})/(H_f - H_{ijk})$ into this expression and evaluation of the integral yields

$$\bar{\rho}^c_{ijk} = \rho^c_{ijk} + \frac{1}{2} \frac{\rho_f - \rho^c_{ijk}}{H_f - H_{ijk}} \left(H_{ijk+1} - H_{ijk} \right).$$

This equation can be rewritten as

$$\bar{\rho}^c_{ijk} = \frac{1}{2}\left(\rho^c_{ijk} + \rho^c_{ijk+1}\right) \tag{12}$$

Case 2) ($H_{ijk} \geq H_f$). If the coolant is boiling for all z in a given node, the assumption is made that its specific volume $1/\rho^c$ increases linearly with enthalpy, which in turn increases linearly with position. In this case, ρ^c_{ijk} is given by

$$\rho^c_{ijk} = \left[\frac{1}{\rho_f} + \frac{1/\rho_g - 1/\rho_f}{H_g - H_f}\left(H_{ijk} - H_f\right)\right]^{-1} \tag{13}$$

where ρ_g and H_g are the density and enthalpy of the saturated vapor, and where possible superheating of the coolant is neglected. The average coolant density in node (i,j,k) may then be computed from

$$\bar{\rho}^c_{ijk} = \frac{1}{H_{ijk+1} - H_{ijk}} \int_{H_{ijk}}^{H_{ijk+1}} \left[\frac{1}{\rho_f} + \frac{1/\rho_g - 1/\rho_f}{H_g - H_f}\left(H - H_f\right)\right]^{-1} dH .$$

Evaluation of the integral in this expression and use of Eq. (13) yields

$$\bar{\rho}^c_{ijk} = \frac{\ln\left(\rho^c_{ijk} / \rho^c_{ijk+1}\right)}{1/\rho^c_{ijk+1} - 1/\rho^c_{ijk}} \quad . \tag{14}$$

Case 3) ($H_{ijk} < H_f < H_{ijk+1}$). For nodes in which boiling begins, the coolant density is assumed to decrease linearly with enthalpy for the portion of the node that is subcooled; whereas the specific volume is assumed to increase linearly with density for the boiling portion. Again, the enthalpy is taken to be a linear function of axial position in the node. The quantity $\bar{\rho}^c_{ijk}$ is thus given by

$$\bar{\rho}^c_{ijk} = \frac{1}{H_{ijk+1} - H_{ijk}} \left\{ \int_{H_{ijk}}^{H_f} \left[\rho^c_{ijk} + \frac{\rho_f - \rho^c_{ijk}}{H_f - H_{ijk}} (H - H_{ijk}) \right] dH \right.$$
$$\left. + \int_{H_f}^{H_{ijk+1}} \left[\frac{1}{\rho_f} + \frac{1/\rho_g - 1/\rho_f}{H_g - H_f} (H - H_f) \right] dH \right\} . \quad (15)$$

Evaluation of the two integrals and simplification of the result yields

$$\bar{\rho}^c_{ijk} = \frac{\alpha}{2} (\rho_f - \rho_{ijk}) + (1-\alpha) \frac{\ln (\rho_f / \rho^c_{ijk+1})}{1/\rho^c_{ijk+1} - 1/\rho_f} \quad (16)$$

where the quantity α is defined as

$$\alpha \equiv \frac{H_f - H_{ijk}}{H_{ijk+1} - H_{ijk}} . \quad (17)$$

Cross section feedback to the neutronic equations is obtained by assuming the cross sections (which are constant throughout the node) to be linear functions of $\bar{T}^f$, $\bar{T}^c$, and $\bar{\rho}^c$ in each node. This linear relation is expressed mathematically as

$$\Sigma^n_{ijk}(I) = \Sigma^n_{ref}(I) + \frac{\partial \Sigma^n(I)}{\partial X} (X_{ijk} - X_{ref}) \quad \begin{cases} X = \bar{T}^f, \bar{T}^c, \text{ or } \bar{\rho}^c \\ \Sigma^n = \Sigma_a, \Sigma_{z1}, \text{ or } \Sigma_f \\ I \rightarrow \text{Composition} \end{cases} \quad (18)$$

where the subscript 'ref' denotes a reference value.

Results

A subroutine TPSSTH (Two Phase Steady State Thermal Hydraulic Feedback) has been written to compute node averaged fuel and moderator temperatures and moderator density using the extended WIGL model. This new subroutine has been added to QUANDRY to allow modeling of BWR's. The proper operation of this subroutine was verified by a number of test problems, one of which is described in detail in the appendix. For this example problem, the global reactor eigenvalue and the normalized power distribution were computed with three different assumptions about the thermal-hydraulic feedback (no-feedback, non-boiling feedback, and boiling feedback) and with two different axial mesh spacings (Δz_k = 15 cm and 30 cm). The effect of these variations on the computed eigenvalue and on the rate of convergence of the outer iteration is shown in Table 1. From this table, it is seen that the cross section feedback both decreases the value of k_{eff} and slows down the convergence of the outer iteration. Both effects are more pronounced for the case in which boiling is allowed. The decrease in k_{eff} is a result of the increase in the diffusion coefficient and the decrease in the fission cross section that accompany a decreasing coolant density and increasing fuel and moderator temperatures. (The increase in leakage rate and decrease in fission rate cause the reactor to become more subcritical.) The larger decrease in k_{eff} for the boiling case is a consequence of the strong variation in $\bar{\rho}^c$ which accompanies boiling. The decreased convergence rate is also completely expected, since the thermal-hydraulic feedback perturbs the existing cross sections and thus delays the approach of the fluxes to their converged values.

The effect of boiling on the reactor power distribution may be examined by plotting, for example, the normalized assembly power density along the line of symmetry given by x=y (i.e. in nodes for which i=j). This distribution is shown in Fig. 1 for the no-feedback case, for the non-boiling feedback model, and for the

Table 1. Variation of the Global Reactor Eigenvalue and the Rate of Convergence of the Outer Iteration with the Type of Thermal Hydraulic Feedback and with Axial Mesh Spacing. The Convergence Criterion for the Eigenvalue, the Initial Eigenvalue Guess, and the Eigenvalue Shift Factor are Constant for all Cases.

Type of Feedback	Number of Axial Mesh Points	Outer Iteration Time (sec)	Eigenvalue, k_{eff}
No Feedback	3	1.5	0.945016
	6	3.5	0.945010
With Feedback (Non-Boiling Model)	3	1.9	0.924382
	6	3.9	0.924197
With Feedback (Boiling Model)	3	3.1	0.917985
	6	5.5	0.917760

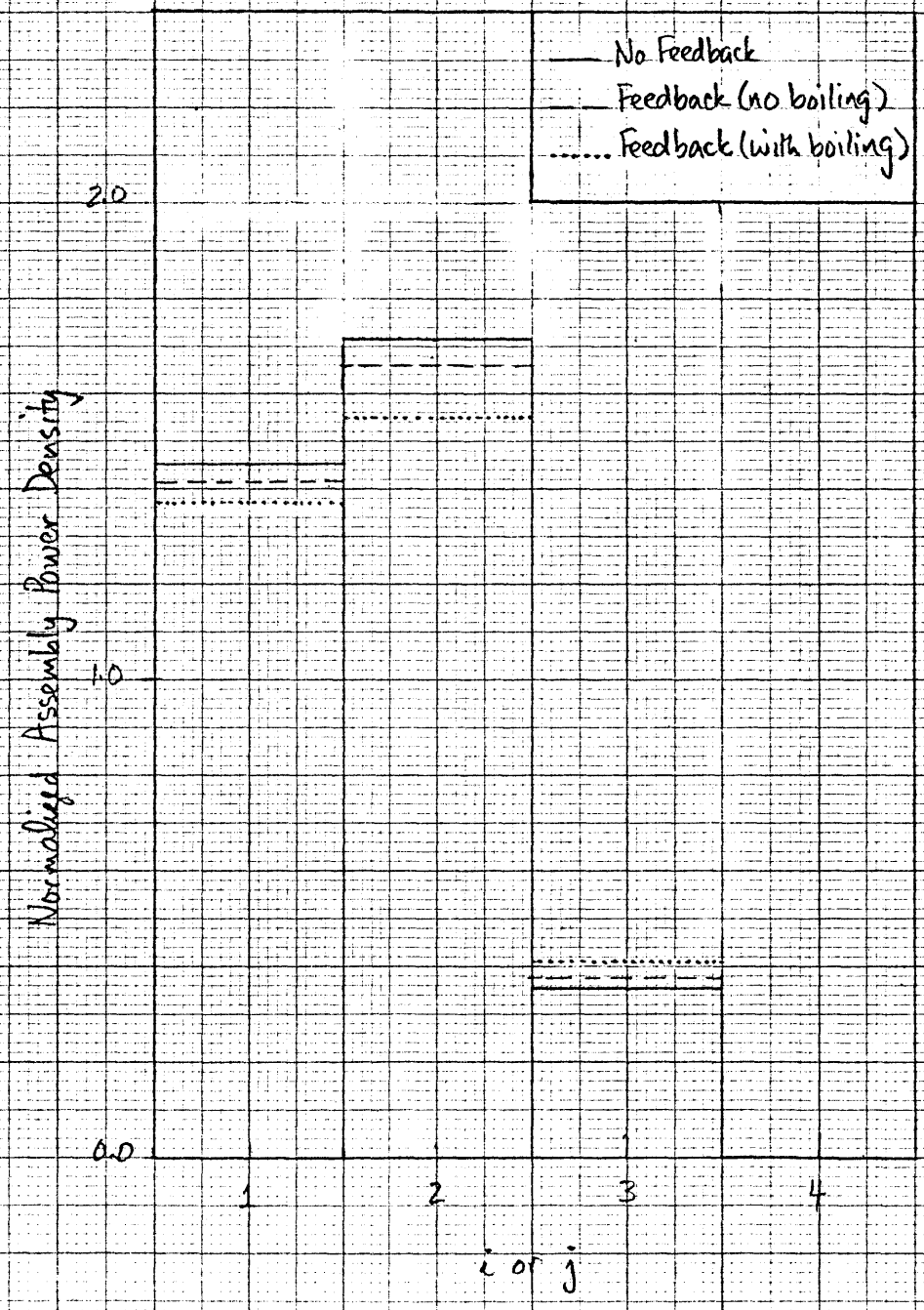

Fig. 1 . Normalized assembly power density along the axis of symmetry (x=y). Three axial nodes were used in each case

boiling feedback model. In this example, it may be seen that the feedback causes the assembly power to decrease in center regions and to increase slightly in boundary regions. This power distribution (flattening) is again completely expected, since regions of higher power are subject to stronger (negative) feedback.

The convergence of the boiling thermal-hydraulic model with respect to spatial discretization can be examined by varying the number of axial nodes and determining the effect on $\overline{T}^f$, $\overline{T}^c$, and $\overline{\rho}^c$ as functions of axial position. First, it was verified that , in the absence of feedback, the neutronic solution for the test problem (given in the appendix) was converged when three axial nodes are used. No changes in k_{eff} and power distribution were observed when the mesh spacing was halved. For comparison, the same axial mesh variation was performed in the same problem with boiling feedback. In this case, only slightly larger changes were observed in k_{eff} and power distribution. Thus it can be assumed that the thermal-hydraulic equations in this example are nearly fully converged with respect to spatial discretization when the same mesh used for the neutronic equations is applied. A comparison of $\overline{T}^t$, $\overline{T}^c$, and $\overline{\rho}^c$ computed with NZ=3 to corresponding values computed with NZ=6 (and collapsed by simple averaging to three-node values) is given in Table 2 for the axial nodes with the line (x,y) = (0,0) at one corner. From this table, it is apparent that the collapsed six-node values are nearly the same as the three-node values, implying that convergence of the thermal hydraulic solutions is nearly achieved using three axial nodes.

Finally, the test problem was run for a case in which the coolant flow rate through the core was halved, and thus boiling occurred at points very close to the bottom (inlet) plane. The increased proportion of coolant which boiled caused additional decreases in k_{eff} and the rate of convergence of the outer iteration. However, even for this severe boiling case, no numerical difficulties were encountered.

Table 2. Effect of the Axial Mesh Spacing on the Axial Variation of the Node Averaged Fuel Temperature $\overline{T}^f$, Moderator Temperature $\overline{T}^c$, and Moderator Density $\overline{\rho}^c$. One node per Interval Corresponds to NZ=3; Two Nodes per Interval Corresponds to NZ=6.

Axial Interval (cm)	Number of Axial Nodes Per Interval	$\overline{T}^f$ (K)	$\overline{T}^c$ (K)	$\overline{\rho}^c$ (gcm^{-3})
0 - 30	1	1644.1	551.3	0.758
	2	1650.6	551.5	0.758
30 - 60	1	1200.7	557.8	0.607
	2	1194.4	557.8	0.592
60 - 90	1	765.1	557.8	0.467
	2	762.5	557.8	0.462

Conclusions

It has been shown that the computer code QUANDRY can be used to obtain consistent solutions for coupled neutronic-thermal-hydraulic problems in LWR's at steady state in which boiling of the coolant takes place. The effect of boiling is primarily to decrease k_{eff} and to flatten slightly the reactor power distribution. Furthermore, even though boiling decreases the rate of convergence of the neutronic solution, convergence can still be obtained for a wide range of conditions that promote boiling. Finally, the thermal-hydraulic solutions converge with respect to spatial discretization when assembly-sized spatial meshes are used, and thus the same mesh used for neutronic solutions can be applied to the thermal-hydraulic part of the overall problem.

Appendix

Description of Test Problem

One problem which was used to test the boiling feedback model is the simple reactor shown in Fig. 2. The reactor composition is assumed constant in the z-direction, and the core is surrounded by 25 cm of water in the x-y plane. Values of the assumed cross sections and cross section coefficients ($\frac{\partial \Sigma}{\partial X}$ in Eq. 18) for each composition in the reactor are given in Table 3. It is noted from this table that the cross section coefficients are assumed to be equal for the two fuel compositions and zero for the reflector composition (i.e. thermal-hydraulic feedback in reflector nodes is neglected).

The coolant pressure is assumed to be uniform and equal to 1000 psi (6.88×10^6 Pa), and the coolant at the inlet plane is assumed to be subcooled by 13K. Numerical values for the input parameters are summarized in Table 4. Zero net current boundary conditions are used for the x=0, y=0, and x=0 planes of the reactor; whereas albedo boundary conditions corresponding to zero incoming partial currents are applied at the outer boundaries of the reactor. The reactor power is taken as 100 MW(t), and the energy release per fission is 3.204×10^{-11} $\frac{\text{Ws}}{\text{fission}}$ (i.e., 200 $\frac{\text{MeV}}{\text{fission}}$).

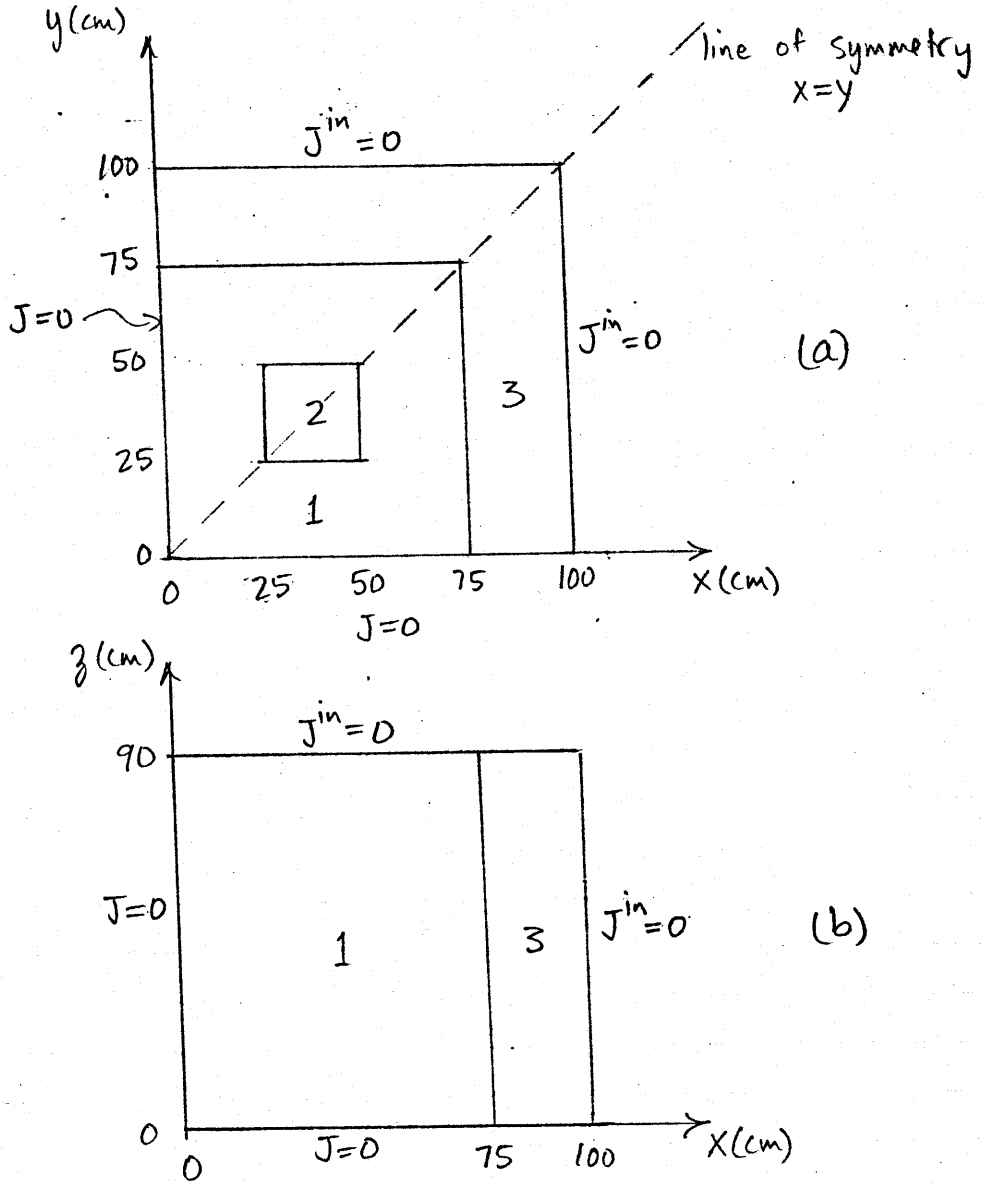

Figure 2. (a) Horizontal reactor cross section at $z=0$
(b) Vertical reactor cross section at $y=0$
The number in each region is the composition number and relates cross sections and cross section coefficients (see table 3) to position.

Table 3. Cross Sections and Cross Section Coefficients for the Compositions Shown in Figure 2

	Cross Section or Cross Section Coefficient - Group 1 followed by Group 2 (cgs units)		
	Composition 1 (ν=2.43)	Composition 2 (ν=2.43)	Composition 3 (reflector)
D	1.255 2.110×10^{-1}	1.268 1.902×10^{-1}	1.257 1.592×10^{-1}
$\partial\frac{1}{D}/\partial\bar{\rho}^{c}$	4.1×10^{-1} 2.7	same as Comp 1 "	0.0 "
$\partial\frac{1}{D}/\partial\bar{T}^{c}$	-8.0×10^{-5} -1.3×10^{-3}	" "	" "
$\partial\frac{1}{D}/\partial\bar{T}^{f}$	-6.6×10^{-6} -2.6×10^{-6}	" "	" "
Σ_t	3.358×10^{-2} 1.003×10^{-1}	3.485×10^{-2} 7.047×10^{-2}	4.184×10^{-2} 1.911×10^{-2}
$\partial\Sigma_t/\partial\bar{\rho}^{c}$	2.683×10^{-2} 5.532×10^{-2}	same as Comp 1 "	0.0 "
$\partial\Sigma_t/\partial\bar{T}^{c}$	1.5×10^{-6} -2.837×10^{-5}	" "	" "
$\partial\Sigma_t/\partial\bar{T}^{f}$	4.15×10^{-7} -2.81×10^{-6}	" "	" "
Σ_{21}	2.533×10^{-2}	2.767×10^{-2}	4.754×10^{-2}
$\partial\Sigma_{21}/\partial\bar{\rho}^{c}$	2.4×10^{-2}	same as Comp 1	"
$\partial\Sigma_{21}/\partial\bar{T}^{c}$	-1.5×10^{-6}	"	"
$\partial\Sigma_{21}/\partial\bar{\rho}^{c}$	8.5×10^{-8}	"	"

Table 3. (continued)

	Composition 1 (ν=2.43)	Composition 2 (ν=2.43)	Composition 3 (reflector)
Σ_f	1.894×10^{-3} 4.49×10^{-2}	1.897×10^{-3} 3.570×10^{-2}	0.0 "
$\partial\Sigma_f / \partial\bar{\rho}^c$	0.0 1.7×10^{-2}	same as Comp 1 "	" "
$\partial\Sigma_f / \partial\bar{T}^c$	0.0 -8.3×10^{-6}	" "	" "
$\partial\Sigma_f / \partial\bar{T}^c$	0.0 -1.0×10^{-6}	" "	" "

Table 4. Thermal Hydraulic Feedback Data
(all units are cgs)

Specific heat of the coolant, ρ^c	5.43×10^7
Inlet coolant mass flow rate, W	2.0×10^6
Inlet coolant temperature, T^b_{ij1}	5.44×10^2
Coolant pressure, p	6.88×10^7
Film coefficient, h_o	3.0×10^7
Conductivity/conduction length of fuel-gas-clad, U	2.5×10^6
Volume fraction of the coolant, $V^c/(V^f+V^c)$	5.59×10^{-1}
Surface area of clad/volume of coolant, A_h	3.0
Fraction of fission energy released in coolant, r	0.0

References

1. A.V. Vota, N.J. Curlee, Jr., and A.F. Henry, "WIGL3 - A Program for the Steady-State and Transient Solution of the One-Dimensional, Two-Group, Space-Time Diffusion Equations Accounting for Temperature, Xenon, and Control Feedback," WADP-TM-788 (February 1969).

2. K.S. Smith, "An Analytic Nodal Method for Solving the Two-Group, Multidimensional, Static and Transient Neutron Diffusion Equation," Nuclear Engineer and S.M. Thesis, Department of Nuclear Engineering, M.I.T., Cambridge, MA (March 1979).